Carbohydrate Research 348 (2012) 47–54

Contents lists available at SciVerse ScienceDirect

Carbohydrate Research

journal homepage: www.elsevier.com/locate/carres

Dynamic stereochemistry of Topiramate (anticonvulsant drug) in solution: theoretical approaches and experimental validation

Mina Ghiasi [a,*], Afsaneh Arefi Oskouie [b], Hamdollah Saeidian [c]

[a] Department of Chemistry, Faculty of Science, Alzahra University, PO Box: 19835-389, Vanak, Tehran, Iran
[b] Department of Basic Science, Faculty of Paramedical, Shahid Beheshti University of Medical Science, Iran
[c] Department of Science, Payame Noor University (PNU), Zanjan, Iran

ARTICLE INFO

Article history:
Received 14 September 2011
Received in revised form 10 November 2011
Accepted 11 November 2011
Available online 19 November 2011

Keywords:
Topiramate
Karplus equation
Coupling constants
2D NMR
QM calculation

ABSTRACT

Topiramate, an antiepileptic drug, was synthesized with an improved protocol and identified by ^{1}H NMR, ^{13}C NMR, ^{1}H–^{1}H COSY, HMQC and HMBC spectrum. In parallel, density functional theory (DFT) using B3LYP functional and split-valance 6-311++G** basis set has been used to optimize the structures and conformers of Topiramate. Also experimental and theoretical methods have been used to correlate the dependencies of ^{1}J and ^{2}J involving ^{1}H and ^{13}C on the C1–C2 (ω) and C1–O1 (θ) torsion angles in the glycosidic part of Topiramate. New Karplus equations are proposed to assist in the structural interpretation of these couplings. Importantly, due to the sensitivity of some couplings, most notably $^{2}J_{H1R,H1S}$, $^{2}J_{C2,H1R}$ and $^{2}J_{C2,H1S}$ values depend on both C–C (ω) and C–O (θ) torsion angles. Analyses of experimental coupling constants for protons on the pyranose ring of Topiramate indicate a twist boat structure for Topiramate in solution. In all calculations solvent effects were considered using a polarized continuum model (PCM).

© 2011 Elsevier Ltd. All rights reserved.

1. Introduction

Epilepsy is a chronic neurological disorder characterized by seizures that result from the sudden, disorderly depolarization of neurons in the brain.[1,2] Anticonvulsant drugs are estimated to be useful in treating 90% of the epileptic patients.[3] Topiramate,[4–9] a sulfamate substituted monosaccharide: 2,3:4,5-bis-*O*-(1-methylethylidene)-β-D-fructopyranose sulfamate, Figure 1, is an anticonvulsant drug marketed worldwide for the treatment of epilepsy and the prophylaxis of migraine. Recently, Topiramate is being used in a growing number of other applications[10] such as treatment of bipolar disorders[11] and post traumatic stress disorders[12] and is investigated for use in treating several other pathologies such as bulimia nervosa,[13] obsessive compulsive disorder,[14] idiopathic intracranial hypertension,[15] neuropathic pain[16], and infantile spasms.[17] This ability is attributed to both its primary chemical structure and its conformation.

As Figure 1 shows Topiramate contains β-D-fructopyranose sulfamate, the exocyclic sulfamatemethyl group which can exist in three staggered orientations (gauch-gauche, gg; trans-gauche, tg; and gauche-trans, gt), Scheme 1. Thus, because of the medical and clinical properties of this compound, studying the conformation in solution is important, especially the interactions involving the exocyclic hydroxymethyl substituted by sulfamate group at this position.

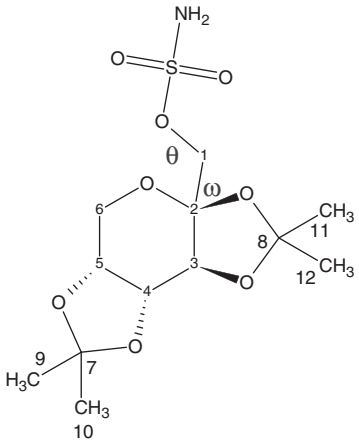

Figure 1. Chemical structure of Topiramate.

So in this study we focused on the sulfamatemethyl ($CH_2OSO_2NH_2$) fragment of fructopyranose in Topiramate to determine its conformation details in solution. Determination of the conformation of biologically active molecules is often based on NMR spectral data in combination with the computational methods.

In the present work, we are interested in extending the use of *J*-coupling constants for the structural, stereo chemical and conformational analysis of Topiramate, by definition of the dependences of $^{2}J_{HH}$, $^{2}J_{CH}$ and $^{1}J_{CH}$ coupling constants on the ^{1}H/^{13}C atomic dihedral angles. So we present the results of the studies of

* Corresponding author. Tel.: +982188044051–9x2608; fax: +982188041344.
E-mail address: ghiasi@alzahra.ac.ir (M. Ghiasi).

0008-6215/$ - see front matter © 2011 Elsevier Ltd. All rights reserved.
doi:10.1016/j.carres.2011.11.010

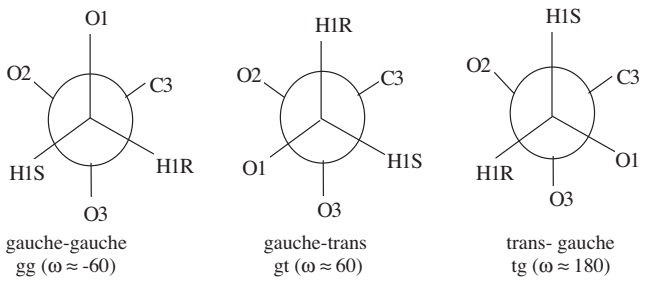

Scheme 1. Idealized rotamers about the C1–C2 bond of Topiramate.

chemical shifts and a set of *J*-couplings about the C1–C2 (ω) and C1–O1 (θ) bonds, $^{2}J_{HH}$, $^{2}J_{CH}$ and $^{1}J_{CH}$, on β-D-fructopyranose, using experimental and theoretical methods to determine the Karplus equation.

2. Experimental

2.1. Synthesis and characterization of Topiramate

The method of preparation involves a two step protocol involving in the first step reacting of 2,3:4,5-bis-*O*-(1-methylethylidene)-β-D-fructopyranose **1** with N-protected sulfamoyl chloride **2** in the presence of triethylamine in toluene to produce N-substituted Topiramate **3**. In the second step hydrolyzing of **3** in pH 3.5 to give Topiramate as a white solid, mp 124–126 °C (Scheme 2).[18]

Step I: *Preparation of N-[(diphenylamino)carbonyl]-2,3:4,5-bis-O-(1-methylethylidene)-β-D-fructopyranose sulfamate* (**3**)

Diphenylamine (1.2 g, 7.1 mmol) in toluene (10 mL) is added dropwise to a solution of chlorosulfonyl isocyanate (1.2 g, 8.5 mmol) in toluene (10 mL) −10 °C under argon. The solution is stirred for 30 min, after which the mixture of 2,3:4,5-bis-*O*-(1-methylethylidene)-β-D-fructopyranose (1.7 g, 6.5 mmol) and triethylamine (1.4 mL, 10 mmol) in toluene is added dropwise. It is then stirred at 5 °C and the progress of the reaction is monitored by TLC. The reaction mixture is washed with water (2 × 15 mL). After separation of the organic layer, is dried over $MgSO_4$, evaporated, and the crude product is used in the next step without further purification.

Step II: *Preparation of Topiramate by the hydrolysis of N-[(diphenylamino) carbonyl]-2,3:4,5-bis-O-(1-methylethylidene)-β-D-fructopyranose sulfamates*

The crude product obtained in step I is dissolved in acetone (7 mL) and sodium acetate–acetic acid buffer solution (pH 3.5). The reaction mixture is heated at 70 °C for 2 h. The cooled mixture is diluted with water (7 mL) and the pH reached upto 13–14 by 10 M NaOH. It is then extracted with *t*-butyl methyl ether (3 × 5 mL). The aqueous phase is treated with 85% phosphoric acid to adjust the pH to 5.5–6 and white crystals precipitate on cooling to 10 °C. The product is collected by filtration and washed with cold water. The purity is increased by recrystallisation from a mixture of acetone and water.

2.2. NMR measurements

^{1}H NMR, ^{13}C NMR, COSY, HMQC and HMBC spectra of Topiramate were obtained at 298 K in $CDCl_3$ (99.99% D) on a Bruker DRX500 operating at 500.133 MHz for ^{1}H and 125.770 MHz for ^{13}C, using 5 mm broad band inverse probe. ^{1}H NMR and ^{13}C NMR spectra were acquired using a spectral width of 3255 and 22123 Hz, respectively, and a 90° pulse (10.3).

All 2D NMR spectra were acquired by pulsed field gradient-selected methods. 2D correlation spectroscopy (COSY) was used to confirm ^{1}H assignments, Figure 2. Heteronuclear multiple quantum correlation (HMQC) and heteronuclear multiple bond correlation (HMBC) were used for ^{13}C assignments, Figures 3 and 4. HMQC and HMBC spectra were recorded using 2048 × 1024 data matrices; the number of scan and dummy scans were 48 and 16, respectively, in all cases.

The HMQC and HMBC were recorded with 2 s inter pulse delay. The spectral widths $sw_1 \times sw_2 = 3255 \times 22123$ Hz in all 2D experiments. For Z-only gradients, the G1:G2:G3 = 50:30:40.1 gradient ratios were used for both HMQC and HMBC spectra.

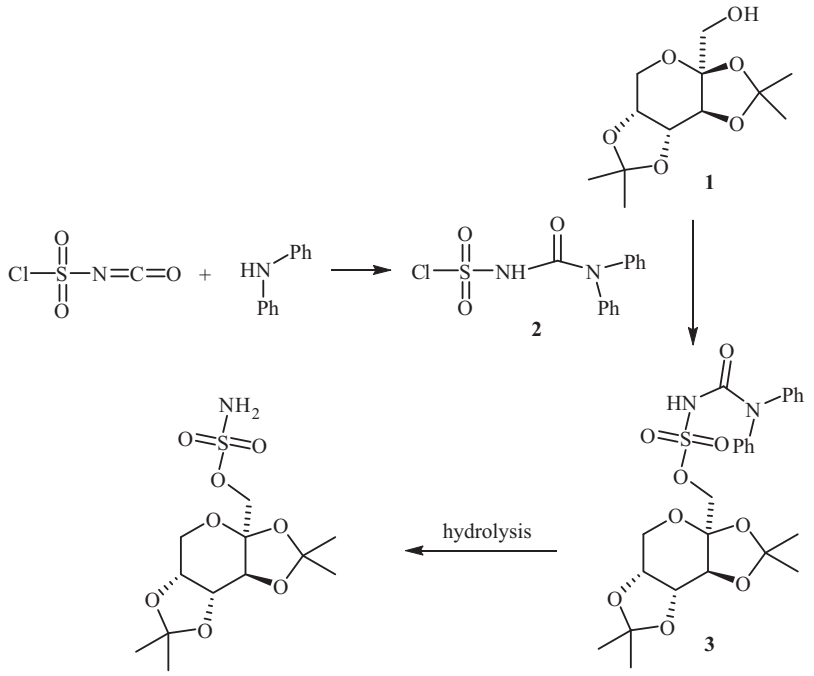

Scheme 2. Synthesis of Topiramate.

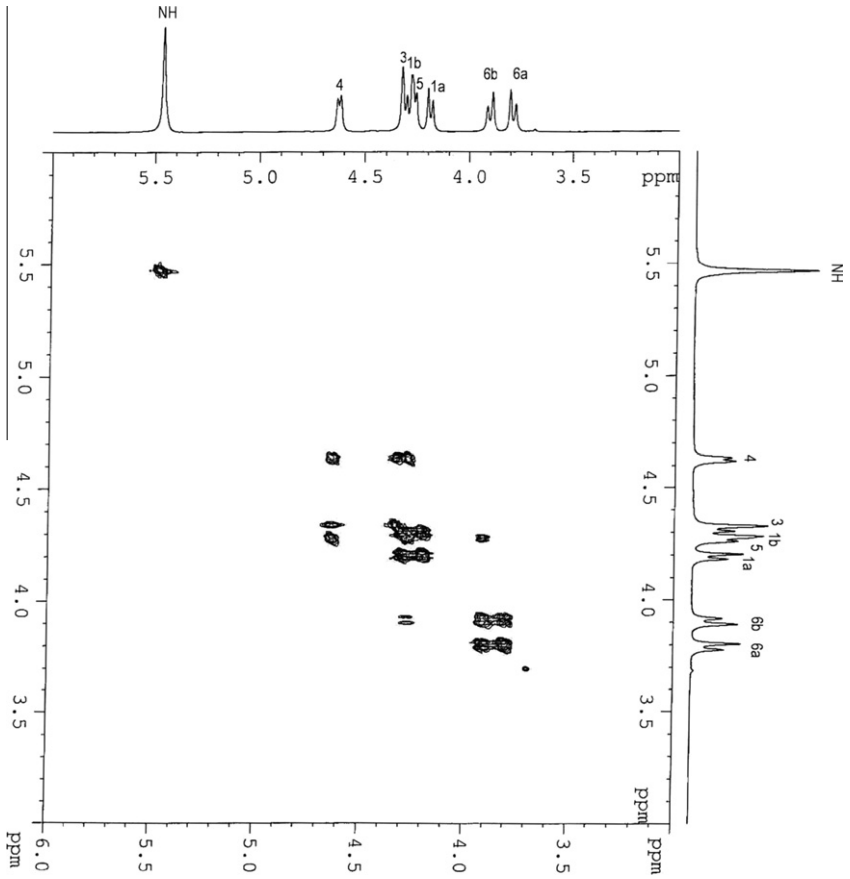

Figure 2. ^{1}H–^{1}H COSY spectrum of Topiramate in $CDCl_3$ at 298 K.

3. Computational details

3.1. Ab initio molecular orbital calculation

All calculations were carried out with GAUSSIAN program series 2003[19] as the basic program and Gaussian viewer as a graphical medium. The optimization of the geometry was performed by employing a hybrid Hartree–Fock density functional scheme and the adiabatic connection method Becke three parameter with Lee–Yang–Parr (B3LYP) functional[20] of density functional theory (DFT)[21] with the standard 6-311++G** basis set. The initial structure of Topiramate was drowning on the basis of published crystal data of Topiramate.[22,23] Full optimizations were performed without any symmetry constrains. This level of theory has been shown to give reasonable potential energy surfaces for D-aldo and D-keto-hexoses and reduces the basis superposition error.[24] We computed the harmonic vibrational frequencies to confirm that an optimized geometry correctly corresponds to a local minimum that has only real frequencies. The solvent effects on the conformational equilibrium have been investigated with a PCM method[25] at the B3LYP/6-311++G** level. Solvation calculations were carried out for $CDCl_3$ with the geometries of optimization for this solvent. Conformational energy profiles around the C1–C2 bond in chloroform were calculated by driving the ω dihedral angle from 0° to 360° in 30° increments, while allowing the remaining geometrical parameters to relax. In this report the orientations about the C2–C1 and C1–O1 bonds are described by torsion angles (ω = O2–C2–C1–O1) and (θ = C2–C1–O1–S) For the C2–C1 rotamers, we used the standard nomenclature, Scheme 1. O2 and C3 are the reference atoms and staggered conformers are designated as gt ($\omega \approx 60$), tg ($\omega \approx 180$) and gg ($\omega \approx -60$).

4. Results and discussion

4.1. Geometry optimization of Topiramate

Topiramate structure was fully optimized in the B3LYP method using 6-311++G** basis set with no initial symmetry restrictions and assuming C_1 point group. The optimized geometry of Topiramate in gas phase was reoptimized by considering the solvent effect (ε = 4.9) using the polarized continuum model (PCM). Tomasi's polarized continuum model defines the cavity as the union of a series of interlocking atomic spheres. The effect of polarization of the solvent continuum is represented numerically.[25] Figure 5 shows the optimized structure of Topiramate in the $CDCl_3$ solvent.

A selection of calculated bond distances, bond angles, and dihedral angles are compiled in Table 1. Calculation of vibrational frequencies has confirmed the stationary point with no negative eigenvalue observed in the force constant matrix.

4.2. Calculation of chemical shifts and NMR spin–spin coupling constants

NMR computations of absolute shieldings were performed using the GIAO method[26] at the DFT optimized structure in the presence of solvent. The ^{1}H and ^{13}C chemical shifts were calculated by using the corresponding absolute shielding calculated for Me_4Si at the same level of theory (Table 2). Good agreement between experimental and theoretical chemical shifts shows the reliability of DFT calculations for these series of molecules.

Recent investigations have shown that density functional theory (DFT) can be used to calculate reliable J_{CH}, J_{HH} and J_{CC} values in carbohydrates without scaling.[27,28] In the present work, we

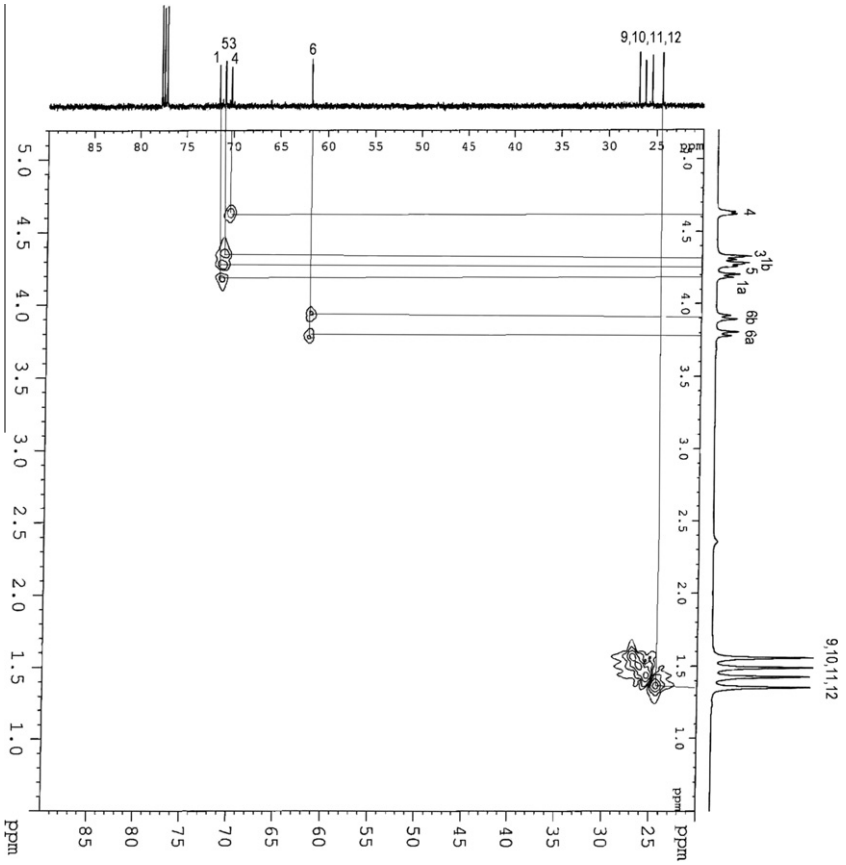

Figure 3. HMQC spectrum of Topiramate in $CDCl_3$ at 298 K.

extend this approach to calculate the *J*-coupling constants using DFT method.

^1H and ^{13}C NMR spin–spin coupling constants in the DFT optimized structure in the presence of solvent were obtained by finite-field (Fermi-contact) double perturbation theory[29] and calculated at the B3LYP level using 6-311++G** basis set. Appropriate values for the perturbing fields imposed on the coupled nuclei were chosen to ensure sufficient numerical precision, while still allowing a satisfactory low-order finite-difference representation of the effect of the perturbation. The result of recent study on heparin, disaccharide with O- or N-sulfated (OSO_3^- or NSO_3^-) residues, show that the Fermi contact (FC) term was not always dominant and that paramagnetic spin-orbit (PSO), diamagnetic spin-orbit (DSO), and spin-dipolar (SD) contributions considerably influenced the magnitudes of proton–proton spin–spin coupling constants.[30] So we consider all the contributions to calculate the coupling constants in the Topiramate molecule. All the equations describing the dependencies of $^2J_{CH}$ and $^2J_{HH}$ on ω and θ were parameterized from the calculated couplings using a least-squares procedure. Specific staggered hydroxymethyl rotamers of Topiramate generated by systematically rotating the (ω = O2–C2–C1–O2) and (θ = C2–C1–O1–S) torsion, from 0° to 360° in 30° increments by holding both the torsion angles at fixed values, were constructed in a Gaussian viewer and subsequently geometrically optimized using B3LYP/6-311++G**. These structures were reoptimized taking solvent effects into account.

4.2.1. Geminal (two bond) ^1H–^1H spin–spin coupling constants

$^2J_{H1R,H1S}$ is affected by both ω and θ, but its dependence on θ is significantly greater than ω. The latter conclusion is supported by previous studies of Stenutz et al.,[31] which shown computed $^2J_{H1R,H1S}$ was related to both ω and θ. The additional hyper surface dataset obtained in this work yielded an improved equation, (Eq. 1), with a substantially smaller rms error. According to Table 3 the following (Eq. 1) is yielded for Topiramate that related $^2J_{H1R,H1S}$ to ω and θ.

$$^2J_{H1R,H1S} = -10.82 + 0.23\cos(\omega) - 0.70\cos(2\omega) - 0.71\cos(\theta) + 1.96\cos(2\theta)(rms = 0.41\,\mathrm{Hz}) \quad (1)$$

The results of the previous study[32–34] show that $^2J_{HH}$ values in unsubstituted CH_2OH fragment influenced both ω and θ, which could be caused by the value of the H–C–H bond angle (this angle appears relatively constant despite changes in ω and θ) on $^2J_{HH}$. So the $^2J_{HH}$ values in the unsubstituted CH_2OH fragment appear to be influenced minimally by the H–C–H bond angle but whether O-substitution affects the H–C–H bond angle significantly. Therefore, this factor may be needed to be considered in the structural interpretation of $^2J_{HH}$.

4.2.2. One bond ^{13}C–^1H spin–spin coupling constants

In previous studies[35–37] it was shown that one-bond proton–carbon couplings usually deviate from experimental data in both directions: inaccuracy in the geometries and neglect of solvation effects. So in this study we used the B3LYP/6-311++g** by considering the solvent effect to decrease the effect of these two items. Hircovíni et al.[37] show that the calculated one bond proton–carbon couplings even using MM2 level of theory are 6–10 Hz smaller than the experimental values (the deviation is about 5% of the experimental values). They show one-bond proton–carbon coupling constants among anomeric protons, similarly the three-bond proton–carbon depended on the torsion angle θ. It seems that the interaction of O atom electron lone pairs with MO of the C–H bond causes this dependence; In particular, the C–H bond length determines this dependence.

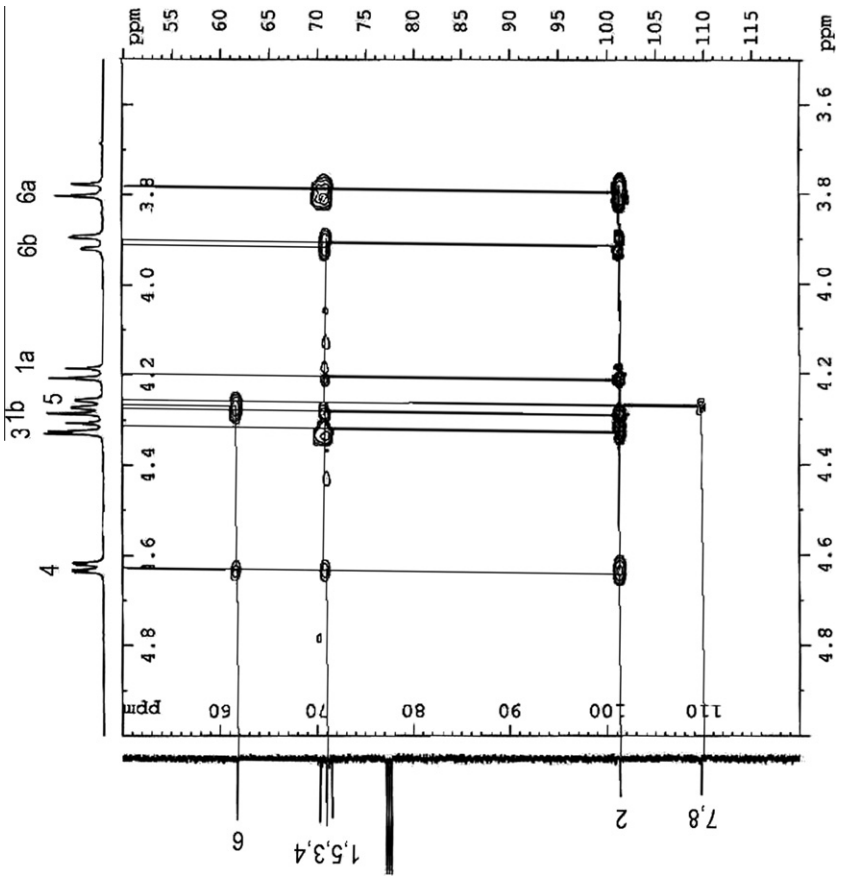

Figure 4. HMBC spectrum of Topiramate in $CDCl_3$ at 298 K.

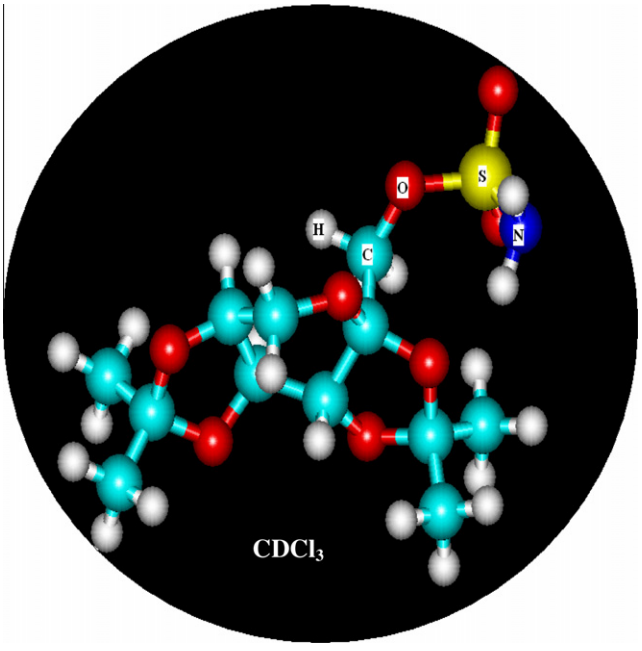

Figure 5. Optimized structure of Topiramate at B3LYP/6-311++G** level in solvent.

Table 1
Some structural details of Topiramate s optimized structure at B_3LYP/6-311++G** level

Bond distance (Å)	
O1–C1	1.43
O1–S	1.65
S–N1	1.66
S–O	1.44
C1–C2	1.54
C2–C3	1.53
C2–O2	1.40
C4–O5	1.41
C10–C11	1.51
Bond angles (degree)	
N1–S–O1	105.36
S–O1–C1	119.93
O1–C1–C2	111.45
C2–O2–C6	114.33
C2–O–C10	109.03
C3–C4–C5	106.32
Dihedral angles (degree)	
N1–S–O1–C1	−90.29
S–O1–C1–C2	92.75
O1–C1–C2–O2	50.69
C2–O2–C6–C5	−33.83

C–H bond length is a key determinant of the $^1J_{CH}$ value, with shorter bond (greater S-character) yielding larger couplings.[32] Several structural factors influence C–H bond length: axial versus equatorial bond orientation, vicinal lone pair effects,[32,38] 1,3-lone pair effect[39], and 1,4-lone pair effects.[31] The shortest C1–H1 bond and the largest $^1J_{C1-H1}$ values, are expected for the C1–H1 bond that does not experience bond-lengthening vicinal (anti) O1 lone-pair interaction and experience bond-shortening 1,3-intraction with an O2 lone-pair. A plot of calculated $^1J_{C1,H1}$ versus r_{C1-H1} is linear, Figure 6, indicating that the C–H bond length is highly correlated

Table 2
Representation of some experimental (in $CDCl_3$ at 298 K) and theoretical chemical shifts (ppm) and coupling constants (Hz) of Topiramate; DFT calculated *J* values in the DFT optimized Topiramate

Chemical shifts					Coupling constant			
^1H	Calcd	Exp.	^{13}C	Calcd	Exp.		Exp.	Calcd*
1(H_R, H_S)	4.15–4.25	4.27–4.37 [a][4.5–4.7]	1, 3, 4, 5	68.5–69.7	70–70.9	$^2J_{H1R,H1S}$	−11.05	−11.4
3	4.12	4.33 [4.28]	2	100.2	101.3	$^2J_{H3,H4}$	2.6	2.8
4	4.38	4.65 [4.4]	3	120.1	117.1	$^2J_{H4,H5}$	7.9	8.1
5	4.17	4.28 [4.24]	6	59.7	61.5	$^2J_{H5,H6}$	0.80	1.0
6(CH_2)	3.65, 3.85	3.82, 3.94 [3.8]		105.3	102.0	$^2J_{H5,H6'}$	2.0	2.1
NH_2	4.58	4.92 [5.2]	CH_3	25.9, 26.8	24.3, 25.5	$^1J_{C1,H1R}$	146.2	146.9
						$^1J_{C1,H1S}$	151.5	152.0
CH_3	1.08	1.19 [1.32]		27.2, 28.1	26.1, 26.8	$^2J_{C2,H1R}$	3.9	4.2
						$^2J_{C2,H1S}$	−4.1	−4.4

[a] Data in parentheses were taken from Abbate et al.[44]

Table 3
Torsion angles, ω and θ (°), and calculated $^2J_{H1R,H1S}$, $^2J_{C2,H1S}$ and $^2J_{C2,H1R}$ values (Hz)

ω	θ	$^2J_{H1R,H1S}$	$^2J_{C2,H1S}$	$^2J_{C2,H1R}$	C1–C2 rotamer
62	57	−12.4	+6.1	−5.2	
57	−48	−11.2	+2.0	−3.4	gt
72	192	−8.9	+2.5	−5.8	
−58	50	−11.5	−2.2	+2.0	
−70	−72	−12.9	−5.0	+6.3	gg
−72	171	−8.6	−5.2	+2.5	
176	74	−11.9	−2.2	−3.5	
177	−69	−12.0	−4.1	−1.6	tg
176	176	−7.3	−4.5	−4.0	
120	60	−12.5	+4.0	−5.5	
120	−60	−12.4	+0.6	−3.5	
120	180	−8.6	−0.3	−5.2	
0	60	−11.5	+3.6	−2.0	
0	−60	11.5	−0.5	+1.7	
0	180	−7.4	−0.5	−2.0	
−120	60	−13.5	−4.0	+1.1	
−120	−60	−13.3	−6.2	+4.8	
−120	180	−9.6	−5.8	+0.5	

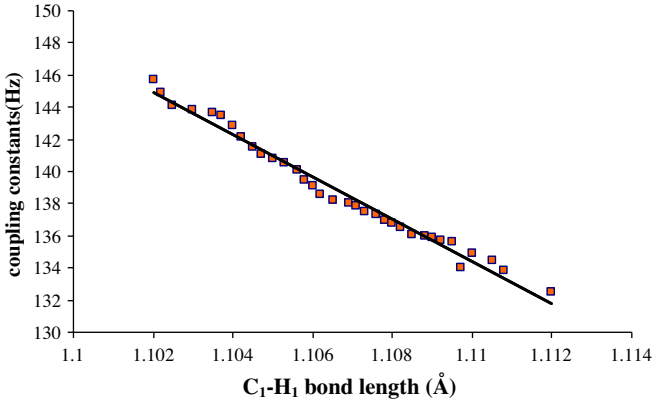

Figure 6. Computed $^1J_{C1H1}$ versus C1–H1 bond lengths, data were generated from systematic rotations about ω and θ.

with $^1J_{CH}$ magnitude, with shorter bonds yielding larger coupling constants. The above results relate the $^1J_{CH}$ to only two torsion angles ω and θ. Rotation of the C1–O1 bond modulates the stereoelectronic effect of the O1 lone-pairs on the C1–H1R and C1–H1S bond lengths, but other effects (1,3-lone pair interactions with O5″ and bond orientation) also influence these bond lengths, so the Karplus equations for Topiramate that relate $^1J_{C1-H1}$ to ω and θ, give relatively large rms errors.

4.2.3. Two bond ^{13}C–^1H spin–spin coupling constants

$^2J_{CCH}$ values are useful structural constraints in biomolecules such as saccharides and nucleosides and their derivatives[40,41] and general rules have been proposed relating $^2J_{CCH}$ to specific patterns of oxygen atom substitution on the coupled carbon and on the carbon bearing the coupled hydrogen. With respect to the CH_2O-SO_2NH_2 conformation, two $^2J_{CCH}$ are expected to be sensitive to ω: $^2J_{C2,H1R}$ and $^2J_{C2,H1S}$. Computed values of these coupling constants are given in Table 3. The dynamic range of $^2J_{CCH}$ is ~+5 to −5 Hz ($\Delta \approx 10$ Hz), and the signs of $^2J_{CH}$ depend on ω.

The dependencies of $^2J_{C5,H6R}$ and $^2J_{C5,H6S}$ on ω and θ were parameterized using the complete dataset of 144 structures from the hyper surface, which yielded (Eqs. 2 and 3).

$$^2J_{C2,H1R} = -1.0845 + 0.99\cos(\omega) - 4.15\sin(\omega) - 1.03\cos(2\theta) - 1.61\sin(2\theta)(\text{rms} = 0.55\,\text{Hz}) \quad (2)$$

$$^2J_{C2,H1S} = 1.12 + 2.15\cos(\omega) + 3.78\sin(\omega) - 0.95\cos(2\theta) + 1.65\sin(2\theta)(\text{rms} = 0.36\,\text{Hz}) \quad (3)$$

4.3. Conformational properties of pyranose ring in Topiramate

According to the Scheme 3 the pyranose ring in Topiramate could exist in three conformations. The critical parameters are the coupling constants of the proton on the pyranose ring: $^2J_{H3,H4}$ = 2.7 Hz, $^2J_{H4,H5}$ = 7.9 Hz, $^2J_{H5,H6}$ = 0.8 Hz, and $^2J_{H5,H6'}$ = 1.9 Hz. For the chair conformation, B, one would expect $^2J_{H3,H4}$ to be a large coupling about 10 Hz 'anti coupling' and $^2J_{H4,H5}$ to be small coupling of 2–3 Hz 'gauche coupling', which is not the case for Topiramate. Alternative chair conformation, C, would exhibit a large coupling for one of the $^2J_{H5,H6}$ values and a small coupling for $^2J_{H4,H5}$. Neither situation is observed in the data for Topiramate. A conformational averaging for Topiramate is probably excluded by large values for the dihedral angle 0 and very small values for $J_{H5,H6}$ and $J_{H5,H6'}$. To confirm twist boat conformation for Topiramate in solution, the geometry of three conformers A, B, and C was optimized, Figure 7, and their coupling constants were calculated in solution. Table 4 indicates some structural details and some calculated proton–proton spin–spin coupling constants in the pyranose ring for these three conformers. Comparison between experimental and calculated coupling constants for the three conformers shows good agreement between conformer A, twist boat, and experimental data. Thus, Topiramate appears to assume a twist boat structure in the solution. A single-crystal X-ray analysis of Topiramate shows a similar twist structure in the solid state.[42]

The results of previous ^1H NMR study in cyclic diacetals of pyranose with 'cis–anti–cis' arrangement[43] and Topiramate[44] tend to adopt a twist-boat conformation, which is in agreement with our results. It appears that the molecule is a combination of a large,

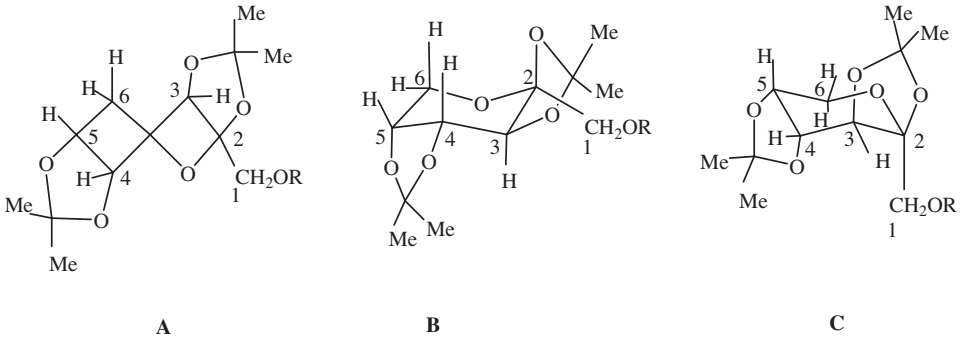

Scheme 3. Presentation of different conformers of Topiramate (R: $S(O_2)NH_2$), A: Twist boat conformer, B: Chair conformer, C: Alternative chair conformer.

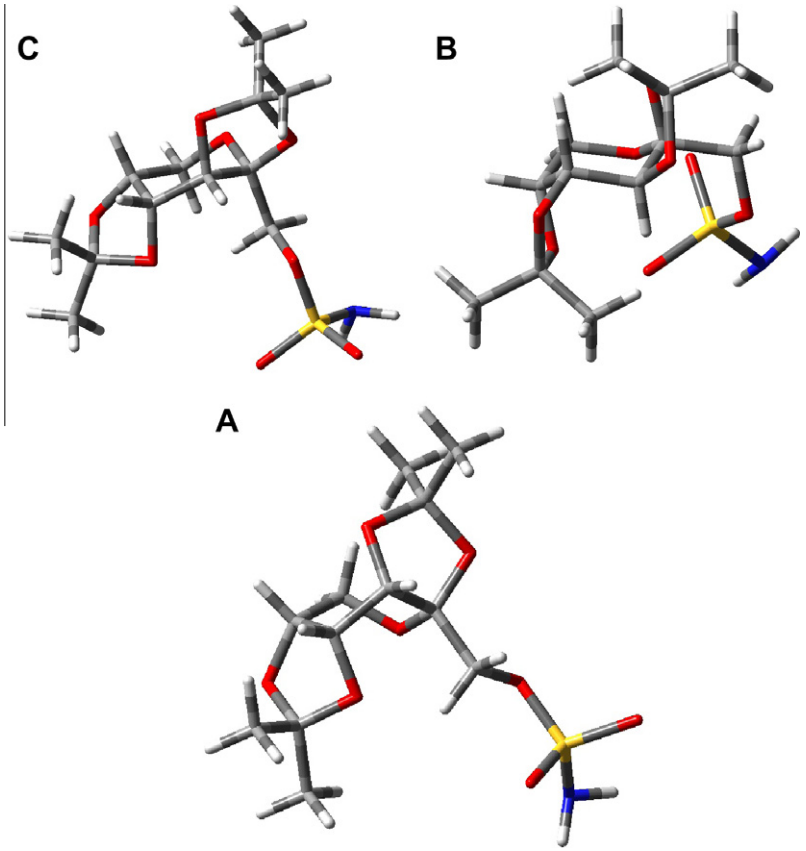

Figure 7. Optimized structure of different conformers of Topiramate (R: $S(O_2)NH_2$), A: Twist boat conformer, B: Chair conformer, C: Alternative chair conformer.

Table 4
Presentation of torsion angles of intra-ring protons and proton–proton coupling constants in pyranose ring for three conformers A, B and C

Conformer	A	B	C	
Torsion angle (°)				
H3C3C4H4	−54.08	176.17	61.07	
H4C4C5H5	176.02	−58.33	55.42	
H5C5C6H6	50.22	54.50	−174.10	
H5C5C6H6′	−86.74	−65.05	−56.50	
Coupling constant (Hz)	Calcd		Exp.	
$^2J_{H3,H4}$	2.8	9.7	2.2	2.6
$^2J_{H4,H5}$	8.1	2.6	1.7	7.9
$^2J_{H5,H6}$	1.0	1.4	9.6	0.80
$^2J_{H5,H6'}$	2.0	2.1	2.0	1.9

globular hydrophobic region and a small hydrophilic SO_2NH_2 unit. We suggest that the nature and disposition of these two segments are important for the biological activity of Topiramate.

5. Conclusion

New structural constraints to assess exocyclic $CH_2OSO_2NH_2$ group conformation in Topiramate based on multiple, redundant *J*-couplings have been described in this report. Using theoretical and experimental methods, equations were developed to correlate the magnitudes and signs of scalar couplings with the CH_2O-SO_2NH_2 conformation. Importantly, some of these couplings display dependence not only on ω but also on θ. More importantly, use of these equations allows assessments of correlated conformation about ω and θ. The strategy was to obtain experimental chemical shifts and coupling constants from Topiramate, and then these data were used to test the ability of DFT methods to estimate the chemical shifts and coupling constants. Good agreement between experimental and theoretical data confirms the accuracy of B3LYP/6-311++G** method for the calculation of chemical shifts and coupling constants of saccharides.

Notice that, the $^{2}J_{HH}$ is determined mainly by the C–O torsion angle (θ) in the absence of a hydroxyl proton on O6, when the hydroxyl group is substituted, (e.g., in a (1→6) glycosidic linkage).

In addition, this report generates new theoretical treatments in drugs with the sugar part which makes the interpretation of saccharide conformational analysis more feasible. These results are expected to be helpful for the understanding of conformational details of Topiramate in solution and give a clue to design binding of Topiramate to DNA molecules and different enzymes. The present findings have significant contribution not only for the studies of Topiramate but also for the related studies of drugs with the saccharide part.

Acknowledgments

The authors gratefully acknowledge partial financial support from the Research Council of Alzahra University. Also the authors would like to appreciate professor Hiroshi Sugiyama from the Tohoku University for his advice and suggestions for this work.

References

1. Trimble, M. R. *New Anticonvulsants Advances in the Treatment of Epilepsy*; Wiley: New York, 1994.
2. Marson, A. G.; Kadir, Z. A.; Chadiwick, D. W. *Br. Med. J.* **1996**, *313*, 1167–1174.
3. Brodi, M. J. *Lancet* **1990**, *336*, 93–96.
4. Bialer, M.; Johannessen, S. I.; Kupferberg, H. J.; Levey, R. H.; Loiseau, P.; Perucca, E. *Epilepsy Res.* **2001**, *43*, 11–58.
5. Stringer, J. L. *Epilepsy Res.* **2000**, *40*, 147–153.
6. Sabers, A.; Gram, L. *Drugs* **2000**, *60*, 23–33.
7. Bourgeois, B. F. D. *J. Child Neurol.* **2000**, *15*, S27–S30.
8. Reynolds, J. E. F. *MARTINDALE, the Extra Pharmacopoeia*, 31 ed.; The Royal Pharmaceutical Society, Council of the Royal Pharmaceutical Society of Great Britain: London, 1996. pp 1652–1680.
9. Casley-Smith, J. R.; Morgan, R. G.; Pillar, N. B.; Engl, N. *J. Med. Chem.* **1993**, *329*, 1158–1163.
10. Mirza, N.; Marson, A. G.; Pirmohamed, M. *Br. J. Clin. Pharmacol.* **2009**, *68*, 655–661.
11. Vasudev, K.; Macritchie, K.; Geddes, J.; Watson, S.; Young, A. Cochrane Database of Systematic Reviews, 2006, Art. No.: CD003384.
12. Berlin, H. A. *Curr. Psychiatry Rep.* **2007**, *9*, 291–300.
13. McElroy, S. L.; Guerdjikova, A. I.; Martens, B.; Keck, P. E., Jr.; Pope, H. G.; Hudson, J. I. *CNS Drugs* **2009**. 23-139-156.
14. Hollander, E.; Dell Osso, B. *Int. Clin. Psychopharm.* **2006**, *21*, 189–191.
15. Celebisoy, N.; Gokcay, F.; Sirin, H.; Akyureki, O. *Acta Neurol. Scand.* **2007**, *116*, 322–327.
16. Bendaly, E. A.; Jordan, C. A.; Staehler, S. S. *Rus. Supp. Cancer Ther.* **2007**, *4*, 241–246.
17. Zou, L. P.; Lin, Q.; Qin, J.; Cai, F. C.; Liu, Z. S.; Mix, E. *Clin. Neuropharm.* **2008**, *31*, 86–92.
18. Arvai, G.; Garaczi, S.; Mate, A. G.; Lukacs, F.; Viski, Z.; Schneider, G. U.S. Patent 20060040874A1.
19. Gaussian 2003 (Revision-B), Frisch, M. J.; Trucks, G. W.; Schlegel, H. B.; Scuseria, G. E.; Robb, M. A.; Cheeseman, J. R.; Zakrzewski, V. G.; Montgomery, J. A.; Stratmann, R. E.; Burant, J. C.; Dapprich, S.; Millam, J. M.; Daniels, A. D.; Kudin, K. N.; Strain, M. C.; Farkas, O.; Tomasi, J.; Barone, V.; Cossi, M.; Cammi, R.; Mennucci, B.; Pomelli, C.; Adamo, C.; Clifford, S.; Ochterski, J.; Petersson, G. A.; Ayala, P. Y.; Cui, Q.; Morokuma, K.; Malick, D. K.; Rabuck, A. D.; Raghavachari, K.; Foresman, J. B.; Cioslowski, J.; Ortiz, J. V.; Stefanov, B. B.; Liu, G.; Liashenko, A.; Piskorz, P.; Komaromi, I.; Gomperts, R.; Martin, R. L.; Fox, D. J.; Keith, T.; Al-Laham, M. A.; Peng, C. Y.; Nanayakkara, A.; Ghonzalez, C. V.; Challacombe, M.; Gill, P. M. W.; Johnson, B. G.; Chen, W.; Wong, M.; Andres, J. L.; Head-Gordon, M.; Replogle, E. S.; Pople, J. A. Gaussian, Inc., Pittsburgh PA, 2003.
20. Beck, A. D. *J. Chem. Phys.* **1993**, *98*, 5648–5652.
21. Parr, R. G.; Yang, W. *Density-functional Theory of Atoms and Molecules*; Oxford Univ. Press: Oxford, 1989.
22. Temperini, C.; Cecchi, A.; Scozzafava, A.; Supuran, C. T. *Bioorg. Med. Chem. Lett.* **2008**, *18*, 2567–2573.
23. Temperini, C.; Innocenti, A.; Mastrolorenzo, A.; Scozzafava, A.; Supuran, C. T. *Bioorg. Med. Chem. Lett.* **2007**, *17*, 4866–4872.
24. Kowalewski, G.; Laaksonen, A.; Root, B.; Siegbahn, P. *J. Chem. Phys.* **1979**, *71*, 2896–2902.
25. Cossi, M.; Barone, V.; Cammi, R.; Tomasi, J. *Chem. Phys. Lett.* **1996**, *255*, 327–335.
26. Wolinski, K.; Hilton, J. F.; Pulay, P. *J. Am. Chem. Soc.* **1990**, *112*, 8251–8260.
27. Bauschlicher, C. W.; Partridge, H. *Chem. Phys. Lett.* **1995**, *240*, 533–540.
28. Cloran, F.; Carmichael, I.; Serianni, A. S. *J. Phys. Chem. A* **1999**, *103*, 3783–3795.
29. Kowalewski, J.; Laaksonen, A.; Root, B.; Siegbahn, P. *J. Chem. Phys.* **1979**, *71*, 2896–2902.
30. Hricovíni, M. *J. Phys. Chem. B* **2011**, *115*, 1503–1511.
31. Stenutz, R.; Carmichael, I.; Widmalm, G.; Serianni, A. S. *J. Org. Chem.* **2002**, *67*, 949–958.
32. Podlasek, C. A.; Stripe, W. A.; Carmichael, I.; Shang, M.; Basu, B.; Serjanni, A. S. *J. Am. Chem. Soc.* **1996**, *118*, 1413–1425.
33. Tafazzoli, M.; Ghiasi, M. *Carbohydr. Res.* **2007**, *342*, 2086–2096.
34. Ghiasi, M.; Taheri, S.; Tafazzoli, M. *Carbohydr. Res.* **2010**, *345*, 1760–1766.
35. Malkin, V. G.; Malkina, O. L.; Salahub, D. R. *Chem. Phys. Lett.* **1994**, *221*, 91–99.
36. Malkina, O. L.; Salahub, D. R.; Malkin, V. G. *J. Chem. Phys.* **1996**, *105*, 8793–8800.
37. Hricovíni, M.; Malkina, O. L.; Bízik, F.; Turi Nagy, L.; Malkin, V. G. *J. Chem. Phys. A* **1997**, *101*, 9756–9762.
38. Kennedy, J.; Wu, J.; Drew, K.; Carmichael, I.; Serjanni, A. S. *J. Am. Chem. Soc.* **1997**, *119*, 8933–8948.
39. Cloran, F.; Zhu, Y.; Osborn, J.; Carmichael, I.; Serianni, A. S. *J. Am. Chem. Soc.* **2000**, *122*, 6435–6448.
40. Church, T.; Wu, J.; Seriani, A. S. *J. Am. Chem. Soc.* **1997**, *119*, 8946–8964.
41. Podlasek, C. A.; Wu, J.; Stripe, W. A.; Bondo, P.; Seriani, A. S. *J. Am. Chem. Soc.* **1995**, *117*, 8635–8644.
42. Maryanoff, B. E.; Nortey, S. O.; Gardocki, J. F.; Shank, R. P.; Dodgson, S. P. *J. Med. Chem.* **1987**, *30*, 880–887.
43. Brady, R. F. *J. Adv. Carbohydr. Chem. Biochem.* **1971**, *26*, 197–202.
44. Abbate, F.; Coet, A.; Casini, A.; Ciattini, S.; Scozzafava, A.; Supuran, C. T. *Bioorg. Med. Chem. Lett.* **2004**, *14*, 337–341.